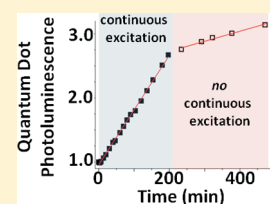


Electron Migration Limits the Rate of Photobrightening in Thin Films of CdSe Quantum Dots in a Dry N₂ (g) Atmosphere

Daniel B. Tice,[†] Matthew T. Frederick,[†] Robert P. H. Chang,[‡] and Emily A. Weiss^{*,†}[†]Department of Chemistry, Northwestern University, 2145 Sheridan Road, Evanston, Illinois 60208-3113, United States[‡]Department of Materials Science and Engineering, Northwestern University, 2220 Campus Drive, Evanston, Illinois 60208-3108, United States Supporting Information

ABSTRACT: This paper describes a study of the mechanism of photoinduced photoluminescence enhancement, termed “photobrightening” (PB), of ~150-nm-thick films of CdSe quantum dots (QDs) in a dry N₂ (g) atmosphere. Steady-state photoluminescence (PL) and ultrafast transient absorption measurements of films photoexcited continuously and shot-wise revealed that: (i) PL enhancement occurred in all of the close-packed films during periods of continuous photoexcitation and continued after the excitation source was turned off; (ii) the time-dependence of PB (both during excitation and in the dark) was initially linear and became exponential as the PB reached saturation; (iii) the rate of PB and the maximum PB achieved by the film depended on the degree of surface passivation of the QDs; (iv) the PL peak shifted to lower energy and broadened during PB; and (v) rates of nonradiative trapping of excitonic electrons decreased during PB. These data were utilized to construct a model for PB based on migration of photoexcited electrons within the film. The basis for this model is that PB is limited by the rate of migration of electrons among surface-localized energetically shallow traps in the film, and *not* by the rate of creation of surface-trapped charge carriers. The migration mechanism provides a rationalization for the seemingly contradictory reports that charging of QD surfaces causes PB in ensembles of QDs but causes photodarkening and blinking in single QDs.



INTRODUCTION

This paper describes a study of the mechanism of photoinduced photoluminescence (PL) enhancement, termed “photobrightening” (PB), of ~150-nm-thick films of CdSe quantum dots (QDs) on glass in a dry N₂ (g) atmosphere. PB results in increases of up to an order of magnitude in the intensity of steady-state PL of QD films and is one of a number of effects, including photoionization^{1,2} and photooxidation,^{3,4} that occur in QDs undergoing continuous photoexcitation.^{4,5} There are reported observations of PB for both core and core–shell CdSe QDs, as well as CdS, PbS, and PbSe QDs.^{6–9} Our observations support previously reported hypotheses^{10–13} that PB originates from the presence of long-lived charged states of QDs. Furthermore, we present evidence for several previously unreported conclusions about the mechanism of PB, namely, that: (i) PB occurs when electrons migrate among shallow traps on QD surfaces throughout the film and inhibit nonradiative electron-trapping processes on proximate QDs and (ii) the rate of PB is limited by the rate of migration of electrons among these shallow traps and not by the rate of creation of surface-trapped charge carriers. Our migration mechanism provides a rationalization for the seemingly contradictory results that charging of QD surfaces causes PB in ensembles of QDs but causes photodarkening and blinking in single QDs.¹⁴

By studying PB in films in a “dry”, N₂ (g) atmosphere—where we define “dry” as <0.1% relative humidity, or ~18 ppm of water at room temperature—we eliminated a number of possible

mechanisms facilitated by some combination of water and oxygen that saturate the PB effect often within tens of minutes.^{3,5,15–17} We were therefore able to observe a regime in which the PL increased linearly in time and a clear shift to a regime where it increased exponentially in time. We used a tandem steady-state PL/transient absorption (TA) setup to monitor simultaneously the time dependence of: (i) the magnitude, energy, and line shape of the films’ PL and (ii) the rate constants for nonradiative decay processes of the QD excitonic state. Unlike PL measurements, TA yields direct information about the evolution of the excited state and the ground state of the entire population of QDs in the film, not just the small fraction emitting light,^{5,18} and thus allows us to determine the effect of continuous excitation on the evolution of nonradiative processes that influence PB. We note that our source of “continuous” excitation to brighten the films is not a continuous-wave light source but rather a 1-kHz pulsed laser (chopped to 500 Hz).

We observed that: (i) PL enhancement occurred in all of the close-packed films that we studied during periods of continuous photoexcitation and *continued after the excitation source was turned off*; (ii) the time dependence of PB (both during excitation and in the dark) was initially linear and became exponential as the PB reached saturation; (iii) the rate of PB and the maximum PB achieved by the film depended on the degree of surface

Received: January 18, 2011

passivation of the QDs; (iv) the PL peak shifted to lower energy and broadened during PB; and (v) rates of nonradiative trapping of excitonic charge carriers decreased during PB. We used these data to construct a model and a descriptive mechanism for PB based on migration of photoexcited charge carriers within the film. This work is a step toward designing QD films to maximize the photobrightening effect and thereby exploit the light-emitting and charge-storage capabilities of solid state devices based on QDs and other nanostructures. It also suggests that, during minutes-long spectroscopic experiments, the optical and electronic properties of nanostructured systems (whether they be films of QDs, metal nanoparticles, or polymers) could be evolving, even if the sample is not continuously photoexcited.

Background. *Trapping of Charge Carriers in Surface-Localized States in CdSe QDs.* QDs are semiconductor nanocrystals with a diameter on the order of the Bohr exciton radius of the bulk material (~ 6 nm in CdSe¹⁹). A large percentage of the atoms of the QD interact with the surrounding medium;²⁰ for example, approximately 56% of the atoms in a 3-nm diameter CdSe QD are at the surface.^{21,22} Incompletely coordinated metal ions at the surface that are not passivated by organic ligands create midgap states that act as traps for the excitonic charge carriers. Within a CdSe nanocrystal, where Cd²⁺ and Se²⁻ are four-coordinate, a Cd²⁺ on the surface that has only two or three bonds to Se²⁻ is a potential electron trap.

Charge trapping is a nonradiative decay process that competes with direct radiative recombination (PL) from the excitonic state. One way to determine the rates of charge-trapping processes is to fit the dynamics of recovery of the ground state bleach, which is a prominent negative feature in the visible transient absorption spectrum. Bleaching of the ground state is induced when population of the 1S_e electron level (analogous to the lowest-unoccupied molecular orbital (LUMO) of a molecule) by the pump beam inhibits subsequent transitions across the bandgap upon excitation with the visible probe beam. The recovery of this bleach is due primarily to depopulation of electrons from the 1S_e state, either by recombination with a hole on the nanosecond time scale or by surface-mediated electron-trapping processes on the picosecond time scale.²³ We obtained time constants for electron trapping processes by fitting the bleach recovery dynamics with a sum of exponentials.²⁴

Photobrightening in CdSe QDs. It is widely agreed upon that PB occurs through inhibition of nonradiative trapping of excitonic charge carriers,^{6,25} but there are many proposed mechanisms for this inhibition, including photoinduced annealing of ligands and the semiconductor lattice at the surface,^{6,26,27} sacrificial oxidation and reduction of surface atoms,⁴ quenching of trapped surface charges,²⁸ chemical reactions involving the native surface ligands,²⁹ passivation of defect sites by the photoinduced adsorption of molecules,^{5,30–33} and photoelectrification, where trapped charges create an electrostatic barrier to trapping upon subsequent excitation.^{10–12,34} Water is commonly implicated in PB as a photoadsorbed ligand that passivates charge-trapping surface defects,^{28,32,33} but photoadsorption of water as the sole mechanism of PB is inconsistent with observations of PL increases in dry atmospheres (including the current report).^{10,12,28}

The photoelectrification mechanism relies on the dissociation of excitons into constituent charge carriers, where one carrier is localized on the surface of the QD and the other is contained in the core, and migration of the surface-localized carrier away from the QD to create long-lived charge-separated (CS) states. Migration of charge carriers results in charging of neighboring

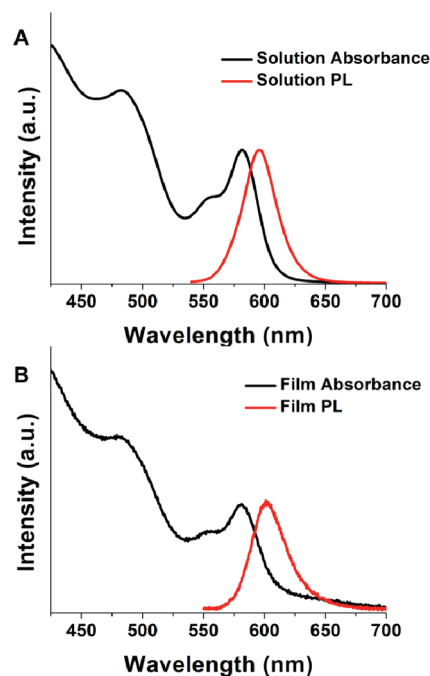


Figure 1. Representative normalized absorption (black lines) and PL (red lines) spectra of the CdSe QDs used for all experiments in this study in both solution (A) and film (B). The maximum of the first absorption feature for both film and solution was at 581 nm, which corresponds to a diameter of 3.9-nm, and the maximum of the PL peak was 596 nm for the solution sample and 602 nm for the film sample. The bathochromic shift and broadening of the PL in the film indicates energy transfer to the largest QDs in the close-packed film.

QDs. If the migrating charge carrier is an electron, then this charging inhibits subsequent electron trapping processes on proximate QDs by increasing the average energy of surface-localized trap states. For QDs in which electron trapping is the primary process competitive with radiative recombination, photoelectrification decreases the probability of trapping, increases the probability of PL, and brightens the film.

The photoinduced charging of QDs has been measured directly through electrostatic force microscopy.^{1,35} Importantly, both charging and brightening of QDs in thin films decay on the time scale of hours once the excitation is removed.^{1,35,36} The knowledge that continuous excitation does, in fact, produce long-lived CS states, and that the charging and PB processes decay on similar time scales, suggests that the two processes (charging and PB) are related, and that the photoelectrification mechanism is responsible for PB. A causal relationship between charging and PB has not been definitively established, however, because many researchers have linked long-lived charged states to dark states—that is, the OFF periods within the PL blinking trajectories of single QDs.^{1,3,25,34,35,37,38} These OFF periods occur when the charge carrier trapped in the core participates in a nonradiative Auger process, by which the energy from recombination of a new exciton is used to thermally excite the core-bound carrier rather than being emitted as a photon.^{11,25,34} Here, we provide evidence that photoelectrification is, in fact, operative in the PB of films of CdSe QDs, and that the seemingly contradictory observations that charging of QDs causes both brightening and darkening can be rationalized by a mechanism in which surface-trapped charge carriers migrate through the film to brighten QDs that do not contain Auger-inducing core charges.

EXPERIMENTAL METHODS

Preparation of Films of CdSe QDs. To synthesize 3.9-nm CdSe QDs, we used a procedure by Qu et al. with slight modifications.³⁹ The Supporting Information contains details of the synthesis and purification. To prepare films of QDs, we thoroughly rinsed a 1.4 cm × 1.4 cm × 0.12 cm portion of a glass microscope slide (VWR) sequentially with chloroform, methanol, and acetone and dried the substrate under a N₂ gas flow. We then spun-cast four drops of a purified $(2.4 \pm 0.1) \times 10^{-5}$ M solution of QDs in hexanes onto the substrate (500 rpm for twenty seconds before ramping to 3000 rpm for an additional thirty seconds) and placed the substrate into a vacuum oven at 24'' of Hg and 120 °C for six minutes to remove residual solvent. We recorded a ground state absorption spectrum (Cary 5000 UV/vis/NIR Spectrometer) of the resulting films and placed them in the dry N₂ (g) atmosphere used for the PB experiments within three minutes of preparation to minimize uncontrolled exposure to oxygen, light, and water. Figure 1 shows the absorption and emission spectra of the 3.9-nm QDs used in these experiments in both a solution and a film.

Tandem PL/TA Experiments. All experiments were conducted in a home-built gas flow chamber (4'' × 4'' × 8''). We passed N₂ (g) through a Drierite cartridge prior to its entering the sample chamber and continuously purged the dried N₂ (g) through the flow chamber to minimize humidity and oxygen (the relative humidity was $\leq 0.1\%$, as measured with a digital hygrometer (VWR)). We observed no hypsochromic shift of the ground state absorption of the QDs during PB, which would be expected if corrosion of the QDs occurred during the experiment, so the dried N₂ (g) prevented the photo-oxidation of the films of CdSe QDs. The films were exposed to a 15-min dry N₂ (g) purge in the dark prior to any photoexcitation. We note that while we cannot completely eliminate water from these experiments, we show, in the Supporting Information, that the trace water present in the chamber (~ 18 ppm at room temperature) is at least a factor of 100 lower than the concentrations of water that affect PB kinetics.

The excitation source for the PB experiments, and for the TA and PL measurements, was the tunable output from an optical parametric amplifier (OPA, TOPAS-C, Light Conversion), pumped by the 1-kHz repetition rate, 795-nm output of a mode-locked, regeneratively amplified Ti:Sapphire laser with an IRF of 100 fs (Solstice, Spectra Physics). The output from the OPA was halved to 500 Hz using a chopper wheel to allow for active background subtraction and generate a differential absorption spectrum. Unless noted, we tuned the power of the laser to achieve an excited state expectation value of 0.20 ± 0.01 , as measured by the ΔA of the ground state bleach in the TA spectrum.

The probe for the TA experiments was a white light continuum generated by focusing a portion of the 795-nm output of the laser through a sapphire plate; this beam was collimated and focused into a fiber optic connected to a charge-coupled device (CCD) array detector after passing through the sample. The probe spot was slightly defocused on the sample to minimize thermal damage to the films. The PL from the film was collected and focused onto an additional fiber optic that was connected to another CCD detector (Jaz, Ocean Optics). We excited the films through the glass and angled them $\sim 20^\circ$ off-normal to the pump beam in order to collect the PL, and to minimize scattering of the pump light into the PL detector. The Supporting Information contains a schematic diagram of the optical excitation and detection setup.

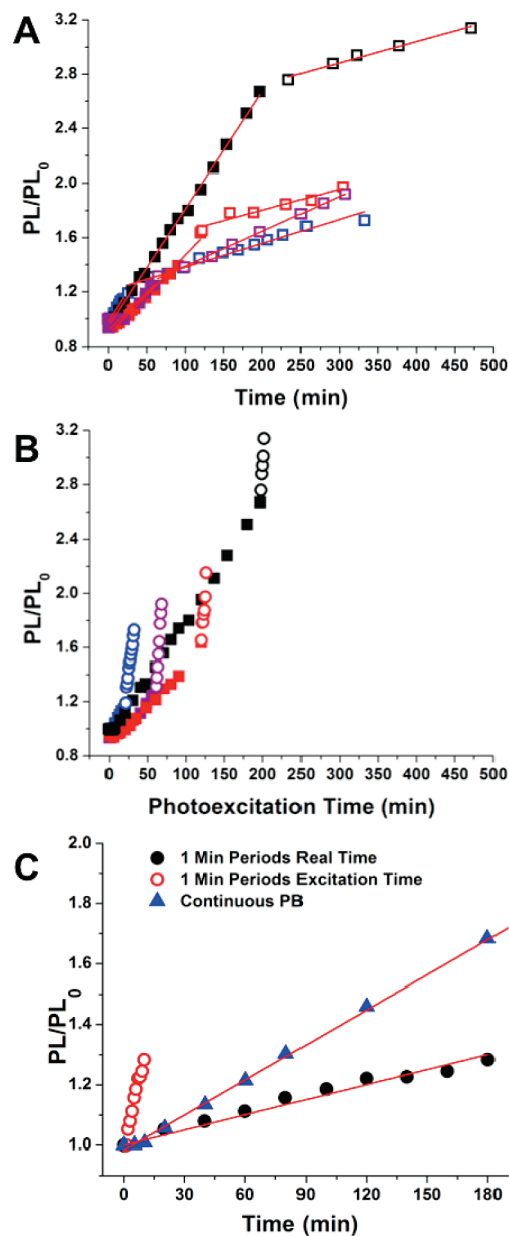


Figure 2. (A) Plots of PL/PL₀ vs real time for four films, continuously photoexcited for different periods of time (solid squares) and subsequent shotwise measurements of PL/PL₀ (open squares). The red lines are fits of the data to eq 7. The slopes during continuous PB and shotwise PB are included in the Supporting Information. (B) The same values of PL/PL₀ as in Figure 2A but plotted against photoexcitation time; these plots show that the brightening observed by the shotwise measurements cannot be due only to the photoexcitation used to acquire the PL spectra. (C) Plots of PL/PL₀ for a film excited shotwise in one-minute periods at 19-min intervals over three hours vs real time (black solid circles) and vs photoexcitation time (red open circles). For reference, the solid blue triangles are a plot of PL/PL₀ for an identical film that was continuously photoexcited for three hours. The red lines are fits of the linear regime with eq 7 (fitting parameters in the Supporting Information).

RESULTS AND DISCUSSION

After Initial Photoexcitation, Brightening of QD Films Occurs in the Dark. Figure 2A shows plots of the integrated PL intensity divided by the initial integrated PL intensity (PL/PL₀) vs time for four films of 3.9-nm CdSe QDs for which the PL

magnitude increased linearly in time over the period that we monitored the films.

The solid squares in Figure 2A are measurements of PL/PL₀ during continuous excitation—that is, where the laser was on continuously during and between PL measurements. We continuously photoexcited the films for varying lengths of time: 20 min, 1 h, 2 h, and 3 h. The slope of PL/PL₀ during continuous photoexcitation varied with the passivation of the surfaces of the QDs within the film, as we discuss later in this paper. The open squares are measurements of the PL/PL₀ during subsequent shotwise excitation—that is, where the laser was off for 19 min between one-minute periods during which it was on in order to acquire the PL spectra. During the off-times, the sample was isolated from all stray light. During shotwise excitation, the PL of the films *continued to increase linearly*, albeit with a smaller slope than during the continuous excitation.

Figure 2B shows that the brightening that occurred during shotwise excitation (“dark brightening”) *cannot* be accounted for by the one-minute periods of photoexcitation used to acquire the PL spectra. If these one-minute periods of photoexcitation were solely responsible for the observed PB, then plots of PL/PL₀ vs photoexcitation time (rather than real time) would have the same slope as those for continuously excited films. We see from Figure 2B, however, that plots of PL/PL₀ vs photoexcitation time under shotwise excitation are steeper than plots for the same films under continuous photoexcitation, by factors of 5, 16, 12, and 11 for the 20-min, 1-h, 2-h, and 3-h photoexcitation periods, respectively.

Figure 2C (black solid circles) shows a plot of PL/PL₀ for a film that was never excited continuously, but rather shot-wise from the start of the experiment. We photoexcited the film for one-minute periods every 20 min for 3 hours. This film brightened over the length of the experiment, with a smaller slope than an identically prepared film that was excited continuously over the 3-h period (blue triangles). Again, plotted against excitation time rather than real time (red open circles), the slope of the film excited shotwise is 7.8 times larger than that excited continuously.

The data in Figure 2 show conclusively that, although some photoexcitation—usually one minute or less—is necessary to initiate the PB process, PB occurs on the order of hours (up to six hours in our study, see Supporting Information) in the dark, *without* creation of new charge carriers in the film. This result proves that another mechanism, in addition to creation of charge carriers, is responsible for brightening the film. Additionally, since the slope of PL/PL₀ is not solely determined by the number of photoexcited QDs, PB cannot be caused by any process—such as photoadsorption of passivating ligands—that has a rate that is dictated solely by the number of photoexcited QDs.

We propose that the mechanism for the increase in PL in the absence of continuous photoexcitation is migration of charge carriers throughout the film by hopping of these carriers from QD surface to QD surface. Inter-QD hopping is a known mechanism for transport of charge carriers through films of CdSe QDs.⁴⁰ We also propose that the charge carriers that cause PB are electrons (rather than holes), since electrons have more spatially delocalized wave functions than holes, and have been observed to be the majority carriers in films of CdSe QDs.^{1,41} The next few sections contain evidence that supports these hypotheses and outline a model for the rate of PB.

We note that, in some cases, a decrease in the PL occurred for between 5 and 20 min before PB began. This decrease was bigger

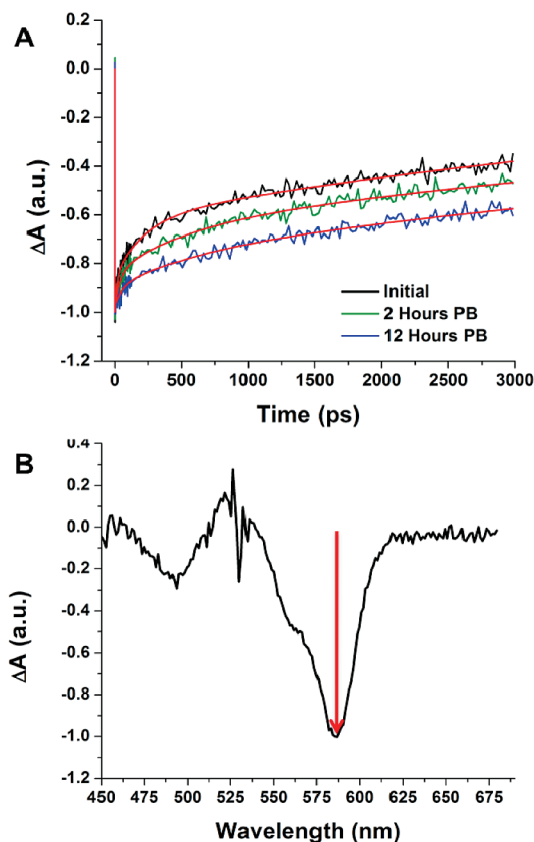


Figure 3. (A) Representative normalized kinetic traces and multi-exponential fits of the recovery of the ground state bleach of a film (PL data for film is in Figure 4) at different times during a continuous photoexcitation period (fitting parameters in Table 1). (B) TA spectrum of same film acquired 2 ps after photoexcitation with 527-nm light. The red arrow indicates the wavelength at which we measured the kinetics in Figure 3A. The feature at 527 nm is scattered pump light.

in magnitude and occurred for longer times for films deposited from solutions of QDs that were exposed to ambient atmosphere for tens of hours prior to spin-casting of the films. We attribute this initial quenching of PL, which is explained in more detail in the Supporting Information, to a hole trapping process enabled by oxidation of the QDs and eventually out-competed by the PB effect. We do not, however, believe that oxidation contributes to the observed PB response in any of our samples because we do not observe the hypsochromic shift of the PL or ground state bleach peaks reported by numerous authors to be associated with photooxidation (and etching of the QD core).^{3–5,16}

Brightening Is Accompanied by a Slowing of Electron Trapping Processes. We observed a ubiquitous decrease of the average rate of recovery of the ground state bleach with continuous and shotwise photoexcitation (Figure 3). This decrease is due to a decrease in the relative amplitudes of the picosecond electron trapping components as well as a lengthening of the time constants for all of the bleach recovery components (Table 1; additional data in Supporting Information). The slowing of the bleach recovery coupled with an increase in PL suggests that PB occurs through inhibition of electron-trapping processes via the photoelectrification mechanism,^{10–12} where a repulsive potential from electrons already present in the film increases the energy required for additional photoexcited electrons to trap into surface sites.

Table 1. Time Constants, τ , And Normalized Amplitudes, A , for the Components of the Multiexponential Fit of the Kinetic Traces for the Ground State Bleach Recovery in Figure 3 at Different Stages in the PB Process^a

| PB time | τ_1 (ps) | A_1 | τ_2 (ps) | A_2 | τ_3 (ps) | A_3 |
|---------|---------------|-------|---------------|-------|-------------------|-------|
| initial | 15 | 0.15 | 220 | 0.24 | 6.1×10^3 | 0.61 |
| 2 h | 40 | 0.13 | 500 | 0.19 | 8.6×10^3 | 0.68 |
| 12 h | 54 | 0.08 | 610 | 0.13 | 1.0×10^4 | 0.79 |

^aThis trend in time constants and amplitudes with PB time is representative of all of the films we examined. The Supporting Information contains data for other films.

The inhibition of electron trapping processes occurs in QDs throughout the film, whether or not they are emissive and contribute to the observed PB. We demonstrated this concept by measuring the TA dynamics of a film of QDs treated with 1-octanethiol (OT), a known trap for excitonic holes, and quencher of PL, in CdSe QDs.²⁴ Upon continuous excitation, this film exhibited a slowing of the bleach recovery to a comparable degree as the films with no OT (see the Supporting Information).

Brightening is Accompanied by a Stark Shift of the PL of the QDs. Figure 4A shows a representative plot of PL/PL₀ vs time for a film in which the PL magnitude initially increased linearly and then trended toward an exponential line shape as it approached a saturation point (here, at PL/PL₀ = 1.75). Figure 4B shows a plot of λ_{max} (triangles) and the full width at half-maximum (FWHM, circles) of the PL peak for this film during continuous (solid symbols) and shotwise (open symbols) photoexcitation. We observed an increase in both λ_{max} and in the FWHM of the PL with a kinetic trace very similar to that for the increase PL/PL₀ in Figure 4A. We interpret the bathochromic shift and initial broadening of the PL during continuous illumination as a charging-induced Stark shift of the PL that accompanies PB.⁴² The broadening occurs because, as PB proceeds, we observe PL from a mixed population of neutral and charged (red-shifted) QDs. These data are consistent with our hypotheses that surface-trapped charges are the origin of PB, that migration of trapped charge carriers contributes to PB under continuous excitation, and that the rate of brightening during dark periods (shot-wise excitation) is dictated by the rate of migration of charge carriers through the film.

The fact that PB is accompanied by a shift in λ_{max} to lower energy provides more evidence that the charge carrier responsible for PB is a migrating electron, not a hole, because a similar configuration, the “negative trion” (negatively charged exciton), has been shown to have lower-energy emission than a neutral exciton. The emission of a positively charged trion is shifted to higher energy from that of the neutral exciton.^{42,43} We observed no hypsochromic shifts in any of our PB experiments. We therefore believe—as expected based on the relative mobilities of holes and electrons in films of CdSe QDs⁴¹ and based on slowing of electron trapping processes seen in the TA data—that the holes remain immobile in primarily nonluminescent QDs, while the electrons migrate through the film and brighten proximate neutral QDs. We note that we observe no change in the position of the ground state bleach (i.e., the absorption wavelength) during the illumination; we believe that the fraction of QDs that are charged is too small to be detected by TA because TA “observes” all of the QDs in the sample, while the PL “observes” only those QDs that are emissive, and therefore is

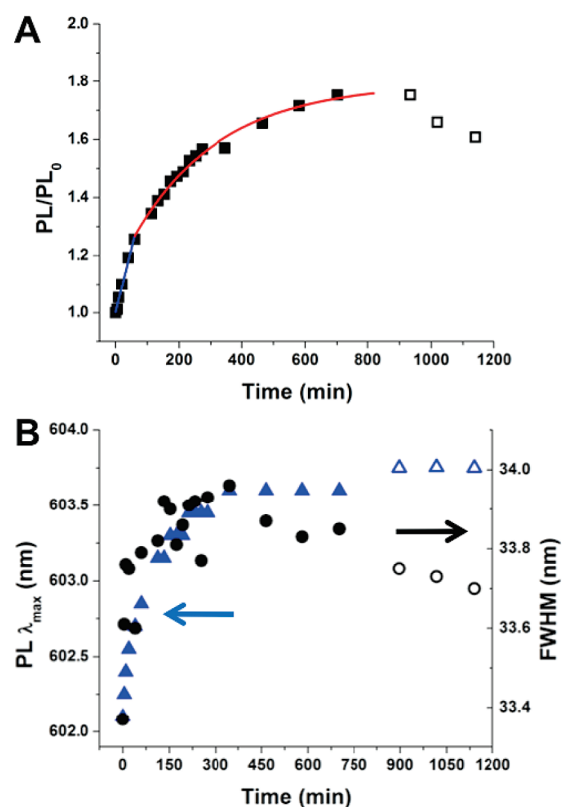


Figure 4. A) Plot of PL/PL₀ for a film of CdSe QDs undergoing continuous photoexcitation until the PL increase approached saturation (solid squares) followed by shotwise measurements (open squares) as the sample sat in the dark. The blue and red lines correspond to fits of the linear and saturation regimes with eqs 7 and 8a, respectively. (B) Corresponding PL peak maximum (blue triangles, left axis) and FWHM (black circles, right axis) of the same film under continuous photoexcitation (solid points) and shotwise measurements (open symbols).

much more sensitive to those QDs that are charged, brightened, and Stark-shifted.

Figure 4A also shows that, for a film in which the PB has saturated, upon removing continuous photoexcitation, the PL decreases (the Supporting Information shows data from an additional film exhibiting this behavior). This decrease cannot be accounted for solely by discharging of the film, because the PL of photobrightened films that had not yet reached saturation *did not decay* when left in the dark for comparable amounts of time. This result indicates that either (i) charges in a film with saturated PL are less stable than in a film that has not reached saturation or (ii) saturation of PL occurs when all accessible potentially bright QDs are already brightened by interaction with charges. In the latter case, decay of PL occurs when these charges begin to migrate away from the brightened QDs.

The mechanism of PL decay is difficult to prove, due to both the long time scale of the decay and the impossibility of measuring the PL magnitude without introducing new charge carriers into the film. Additionally, the observation that, as the PL decays, the bathochromic shift of the PL peak remains suggests that the brightened QDs were initially dark, and the removal of the local charge returns them to a neutral but nonemissive state, while the narrowing of the FWHM indicates that the population of emissive QDs becomes increasingly homogeneous, and that this homogeneous population comprises the charged (brightened)

QDs. The predominance of emission from the brightened QDs could occur from the initial neutral emitters becoming photo-darkened over the course of the experiment.

The Rate of Brightening of a Film, and the Point at which Brightening Saturates, Depend on the Surface Passivation of Its QDs. We observed that films with higher average initial (prebrightening) electron trapping rates, and corresponding lower PL_0 , underwent longer periods of linear brightening before saturation, and brightened faster, than films with lower initial trapping rates (Figure 5, Table 2, and the Supporting

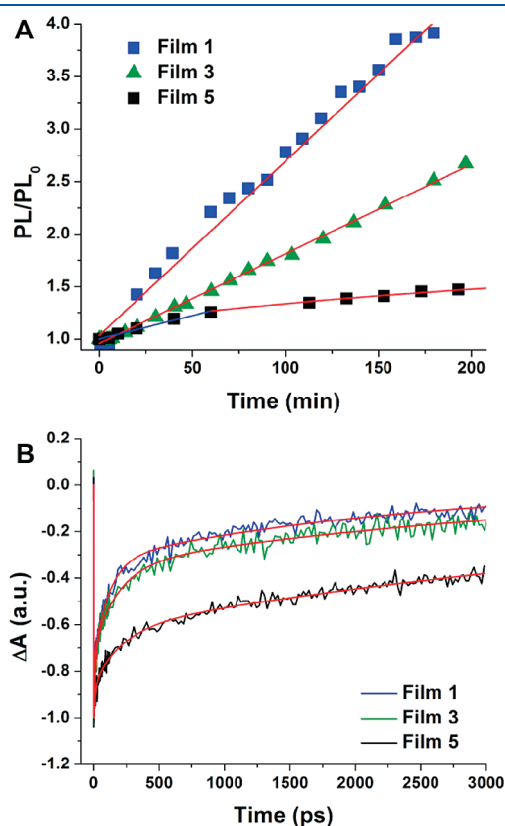


Figure 5. (A) Plots of PL/PL_0 for films 1, 3, and 5 in Table 2 spun from QDs with different initial electron trapping rates, which varied with the time the QDs were stored in a nitrogen glovebox as an unpurified pellet, prior to purification and sample preparation (see Supporting Information). The linear regions of the plots are fit with eq 7, and the exponential regions are fit with eq 8. (B) Normalized kinetic traces of the ground state bleach recovery for these three films at time zero in the plot in Figure 5A (pre-PB). The time constants for ground state bleach recovery were 5.5, 120, and 2.4×10^3 ps for film 1, 14, 190, and 3.3×10^3 ps for film 3, and 15, 220, and 6.1×10^3 ps for film 5.

Information for surface characterization of these films). We believe two factors contribute to these observations. First, the PB mechanism depends on the localization of electrons into deep traps, so the defective films—which have a greater density of QDs with electron traps, in general, and deep electron traps, in particular—sustain brightening for a longer time than do well-passivated films. Second, a defective film will support a higher yield of electron trapping upon photoexcitation. More surface-trapped electrons, as measured by the magnitude of the bleach recovery, translate into faster PB, as measured by the slope of the linear PB curves (Table 2).

Rationalization of the Photoelectrification Mechanism with Previously Observed Photodarkening of Charged QDs. Surface-trapping of charge and subsequent recombination can cause blinking and photodarkening in QDs by creating holes that participate in nonradiative Auger processes. The photoelectrification mechanism for PB does not, however, contradict this picture if the trapped charges brighten *neutral* QDs to which they migrate, rather than charged QDs from which they originate. In other words, the QDs from which the charges originate have holes trapped in their cores and therefore are inherently non-radiative. The PL of these QDs cannot be enhanced by inhibition of electron trapping processes because picosecond Auger processes will always quench their PL. Proximate neutral QDs that do not participate in Auger or other fast nonradiative hole-trapping processes can benefit from the photoelectrification mechanism, and therefore are candidates for brightening by migrating electrons. We propose that brightening occurs when a migrating electron finds a stable trap state (a “deep trap”) within the proximity of a QD for which nonradiative electron trapping is primarily responsible for quenching of the PL, and inhibits the trapping process.

A Mechanism and Model for PL/PL_0 : The Rate of PB is Dictated by the Rate of Electron Migration and Trapping. The following equations constitute a model for PB during continuous and shotwise excitation. We assume that we start with an initial population of QDs for which radiative recombination does not occur only because of the presence of fast, nonradiative electron trapping pathways. Long-lived electrons in deep traps near these QDs inhibit electron trapping and thereby increase the observed PL of the film. The measured change PL/PL_0 in time is therefore proportional to the change in the number density of deep-trapped electrons within a critical distance of one of these potentially bright QDs, $\rho_{\text{dtr-e}}$, eq 1. We assume that the localization of an electron in a

$$\frac{d\left(\frac{PL}{PL_0}\right)}{dt} \propto \frac{d\rho_{\text{dtr-e}}}{dt} \quad (1)$$

Table 2. Comparisons of the Magnitude of the Initial Bleach Recovery with the Slope of the PL/PL_0 vs Time in the Linear Regime of PB^a

| film | initial bleach recovery (%) | slope of PL/PL_0 (PL units/min) | storage time of unpurified QD pellet in glovebox (weeks) |
|------|-----------------------------|-----------------------------------|--|
| 1 | 91% | 0.0170 | used immediately |
| 2 | 87% | 0.0165 | used immediately |
| 3 | 85% | 0.0087 | 2 |
| 4 | 84% | 0.0085 | 2 |
| 5 | 68% | 0.0043 | 5 |
| 6 | 67% | 0.0046 | 5 |

^aThe films in bold type (1, 3, 5) correspond to the films for which the data is shown in Figure 5.

deep trap near a radiative center requires a “collision” between a migrating electron and a deep trap, eq 2, so the value of $d(\rho_{\text{dtr-e}})/dt$ is equal to the product of ρ_e , the number



density of surface-localized electrons migrating through the film, and therefore available to occupy a deep trap, ρ_{dtr} , the number density of deep traps in the vicinity of radiative centers in the film, and k_{dtr} , the rate constant for deep trapping of electrons within the film of QDs, eq 3.

$$\frac{d\rho_{\text{dtr-e}}}{dt} = k_{\text{dtr}}\rho_e\rho_{\text{dtr}} \quad (3)$$

Our experimental data, especially the occurrence of PB in the absence of continuous photoexcitation, suggests that the rate constant k_{dtr} is limited by electron migration through the film. If we define R as the critical distance between a migrating electron and a deep trap at which a trapping event will occur, the migration-limited trapping rate constant, k_{dtr} , is described by eq 4, where D_e is the diffusion constant of the electrons

$$k_{\text{dtr}} = 4\pi D_e R \quad (4)$$

hopping through the film.⁴⁴ Equation 4 assumes that there is no interaction potential between migrating electrons and deep traps (so the rate of trapping is diffusion-limited) and that the deep trap sites are immobile. We can relate D_e to the mobility of the electrons in the film, μ_e , with eq 5, where e is the fundamental charge on the electron, k_B is the

$$D_e = \mu_e \frac{k_B T}{e} \quad (5)$$

Boltzmann constant, and T is temperature (here, 298 K).⁴⁴ Inserting eqs 4 and 5 into eq 3 yields eq 6, where we can group the constants in parentheses into a migration rate

$$\frac{d\rho_{\text{dtr-e}}}{dt} = \left(4\pi R \mu_e \frac{k_B T}{e}\right) \rho_e \rho_{\text{dtr}} = k_{\text{mig}} \rho_e \rho_{\text{dtr}} \quad (6)$$

constant k_{mig} .

In the linear regime of PB, since the trapping process is very slow, neither the population of electrons hopping through the film nor the population of available deep trap sites is significantly depleted, and ρ_e and ρ_{dtr} are effectively constant. Brightening is then gated by a pseudo-zeroth order trapping process (linear in time) with a rate constant dictated by the mobility of electrons through the film. Integrating both sides of eq 6, and assuming all quantities on the right-hand side are constant in time, yields eq 7, which we use to fit the linear regions of the plots in Figures 2, 4, and 5.

$$\frac{\text{PL}}{\text{PL}_0}(t) \propto \rho_{\text{dtr-e}}(t) = (k_{\text{mig}}\rho_e\rho_{\text{dtr}})t \quad (7)$$

(solution for the linear regime)

We observe saturation behavior of PL/PL_0 when the deep traps near radiative centers begin to fill—that is, $\rho_{\text{dtr}} \equiv \rho_{\text{dtr}}(t)$, and k_{mig} and ρ_e are constant, so the trapping process is pseudo-first order, eq 8a, where t_{init} is the time at which the PB curve switches

$$\frac{\text{PL}}{\text{PL}_0}(t) \propto \rho_{\text{dtr-e}}(t) = \rho_{\text{dtr-e}}(t_{\text{init}}) + \rho_{\text{dtr}}(t_{\text{init}})(1 - e^{-Ct}) \quad (8a)$$

$$C = k_{\text{mig}} \times \rho_e \quad (\text{solution for the saturation regime}) \quad (8b)$$

from linear to exponential. The Supporting Information contains a detailed derivation of eq 8a.

This model accounts for PB during both continuous and shotwise excitation. The value of ρ_e is positively correlated with the number of photons absorbed by the film, although we have found that not every photoexcited state of a QD contributes to ρ_e (see Supporting Information). The slope of PL/PL_0 (which is proportional to ρ_e by eq 7) is therefore greater during continuous excitation than during shotwise excitation. The actual value of ρ_e is determined by (i) the photon flux on the sample, (ii) the number of excitons that decay via surface-mediated electron trapping, and (iii) the number of trapped electrons that live long enough to migrate to other QDs before recombining.

The constant value of ρ_e in the linear regime of PL/PL_0 not only implies that the collision of a migrating electron with a deep trap is very slow in this regime (i.e., there is no significant depletion of population of migrating electrons) but also that there is no buildup of population of migrating electrons. We attribute this observation to the vast majority of trapped electrons' recombining with holes before they can migrate to other QDs. In other words, creation of a mobile electron is a rare event (we calculate, in the Supporting Information, that approximately only 1 of every 10^9 electrons excited to the conduction band of the QDs participate in PB); this conclusion accounts for the fact that, despite a rate of excitation of the QDs of 30,000 pulses per minute, some films brighten for tens of hours before reaching saturation.

Although the model described in this section provides a means to quantitatively predict rates of PB, these predictions require measurement and modeling of several parameters describing the film. Determination of values for these parameters is beyond the scope of this work, but the Supporting Information contains the parameters extracted from fits to the plots of PL/PL_0 vs time in both linear and exponential brightening regimes. We are currently exploring independent experiments to quantify these parameters and refine our model for PB.

SUMMARY AND CONCLUSIONS

We found that for thin films of CdSe QD under a dry N_2 (g) atmosphere: (i) creation of charge carriers in the film is not the only process that causes PB, as PB also occurs in the absence of continuous photoexcitation (Figure 2); (ii) PB is associated with an inhibition of electron-trapping processes (Figure 3); and (iii) PB is correlated with bathochromic shifting and broadening of the PL of the QDs (Figure 4). These findings lead us to propose that the mechanism for PB is the inhibition of electron trapping on QDs that do not participate in hole trapping or Auger processes by a coulomb-blockade effect from proximate electrons that have migrated from photoexcited QDs, and that the rate-limiting step for the PB process is this migration of electrons from their point of origin to a deep trap in the proximity of a potentially radiative QD. We modeled the trapping process that causes PB as a “collision” between a migrating electron and a deep trap near one of these QDs in the film. The rate of PB is then dictated by the diffusion constant for the electrons and the number densities of both migrating electrons and deep traps near potentially radiative QDs.

We have shown that PB requires neither an atmosphere of water (or polar vapor) nor continuous photoexcitation. The presence of water in the atmosphere certainly enhances the PB in our films (see Supporting Information), and this enhancement is

probably due to stabilization of charge-separated states by the polar environment. We and others^{28,31} have observed that a large portion of water-facilitated PB is quickly reversible upon drying of the film. We believe that the lack of complete reversibility of water-facilitated PL enhancement indicates the presence of the underlying, quasireversible (or very slowly reversible) dry brightening process that we demonstrate and analyze in this work. The slow rate of dry brightening makes the shape of the PB curve more sensitive to variables such as the surface chemistry of the QDs, interparticle spacing, and the core size of the nanocrystals and therefore enables our study of the influence of these parameters on the PB process.

The unique optical and electronic properties of quantum-confined excitonic materials give them great promise for use as active materials in optoelectronic devices such as LEDs, solar cells, and laser gain media, but a thorough understanding of the evolution of these nominally optically stable systems upon excitation, including changes in their PL, is necessary for the development of efficient and robust materials for these devices. Photobrightening is an excellent example of the influence of the collective behavior of QDs on their optical properties, and shows that PL measurements are a tool for investigating the properties of QD films that allow them to achieve stable charged configurations. If we can identify and manipulate these properties, QD solids have the potential to serve as both a new class of nanoscopic charge storage media, and optical probes of local charging.

■ ASSOCIATED CONTENT

S Supporting Information. Experimental details, derivation of eq 8, examples of fits to PL/PL₀ with eqs 7 and 8, tables of time constants and amplitudes for ground state bleach recovery, data on the effect of laser power, water, and oxygen exposure on PL/PL₀, PB kinetics, and surface chemistry, and Figures S1–S10. This material is available free of charge via the Internet at <http://pubs.acs.org>.

■ AUTHOR INFORMATION

Corresponding Author

*E-mail: e-weiss@northwestern.edu.

■ ACKNOWLEDGMENT

This project was funded by the IGERT: Quantum Coherent Optical and Matter Systems Program (NSF Award number 0801685). The structural characterization of the films was performed in the Keck II and NIFTI facilities of NUANCE Center at Northwestern University. NUANCE Center is supported by NSF-NSEC, NSF-MRSEC, Keck Foundation, the State of Illinois, and Northwestern University.

■ REFERENCES

- (1) Li, S.; Steigerwald, M. L.; Brus, L. E. *ACS Nano* **2009**, *3*, 1267–1273.
- (2) Son, D. H.; Wittenberg, J. S.; Alivisatos, A. P. *Phys. Rev. Lett.* **2004**, *92*, 127406/1–127406/4.
- (3) van Sark, W. G. J. H. M.; Frederix, P. L. T. M.; Bol, A. A.; Gerritsen, H. C.; Meijerink, A. *ChemPhysChem* **2002**, *3*, 871–879.

- (4) Wang, Y.; Tang, Z.; Correa-Duarte, M. A.; Pastoriza-Santos, I.; Giersig, M.; Kotov, N.; Liz-Marzan, L. M. *J. Phys. Chem. B* **2004**, *108*, 15461–15469.
- (5) Cordero, S. R.; Carson, P. J.; Estabrook, R. A.; Strouse, G. F.; Buratto, S. K. *J. Phys. Chem. B* **2000**, *104*, 12137–12142.
- (6) Jones, M.; Nedeljkovic, J.; Ellingson, R. J.; Nozik, A. J.; Rumbles, G. *J. Phys. Chem. B* **2003**, *107*, 11346–11352.
- (7) Miyoshi, T.; Hirano, A.; Suenaga, T.; Nagata, J.; Nagai, T.; Matsuo, N. *Japan. J. Phys. Pt. 1* **2000**, *39*, 6290–6292.
- (8) Peterson, J. J.; Krauss, T. D. *Phys. Chem. Chem. Phys.* **2006**, *8*, 3851–3856.
- (9) Christova, C. G.; Stouwdam, J. W.; Eijkemans, T. J.; Silov, A. Y.; van der Heijden, R. W.; Kemerink, M.; Janssen, R. A. J.; Salemink, H. W. M. *Appl. Phys. Lett.* **2008**, *93*, 121906/1–121906/3.
- (10) Kimura, J.; Uematsu, T.; Maenosono, S.; Yamaguchi, Y. *J. Phys. Chem. B* **2004**, *108*, 13258–13264.
- (11) Uematsu, T.; Kimura, J.; Yamaguchi, Y. *Nanotechnology* **2004**, *15*, 822–827.
- (12) Uematsu, T.; Maenosono, S.; Yamaguchi, Y. *J. Phys. Chem. B* **2005**, *109*, 8613–8618.
- (13) Yu, M.; Van Orden, A. *Phys. Rev. Lett.* **2006**, *97*, 237402/1–237402/4.
- (14) Pelton, M.; Smith, G.; Scherer, N. F.; Marcus, R. A. *Proc. Natl. Acad. Sci. U. S. A.* **2007**, *104*, 14249–14254.
- (15) Wang, W. Y.; Lee, T.; Reed, M. A. *J. Phys. Chem. B* **2004**, *108*, 18398–18407.
- (16) Nazzal, A. Y.; Wang, X.; Qu, L.; Yu, W.; Wang, Y.; Peng, X.; Xiao, M. *J. Phys. Chem. B* **2004**, *108*, 5507–5515.
- (17) Gomez, D. E.; van Embden, J.; Mulvaney, P.; Fernee, M. J.; Rubinsztein-Dunlop, H. *ACS Nano* **2009**, *3*, 2281–2287.
- (18) Jha, P. P.; Guyot-Sionnest, P. *J. Phys. Chem. C* **2007**, *111*, 15440–15445.
- (19) Millo, O.; Katz, D.; Steiner, D.; Rothenberg, E.; Mokari, T.; Kazes, M.; Banin, U. *Nanotechnology* **2004**, *15*, R1–R6.
- (20) Garrett, M.; Bowers, M. J.; McBride, J. R.; Orndorff, R. L.; Pennycook, S. J.; Rosenthal, S. J. *J. Phys. Chem. C* **2008**, *112*, 436–442.
- (21) Murray, C. B.; Kagan, C. R.; Bawendi, M. G. *Annu. Rev. Mater. Sci.* **2000**, *30*, 545–610.
- (22) Bischof, T.; Ivanda, M.; Lermann, G.; Materny, A.; Kiefer, W.; Kalus, J. *J. Raman Spectrosc.* **1996**, *27*, 297–302.
- (23) Sewall, S. L.; Cooney, R. R.; Anderson, K. E. H.; Dias, E. A.; Sagar, D. M.; Kambhampati, P. *J. Chem. Phys.* **2008**, *129*, 084701/1–084701/8.
- (24) McArthur, E. A.; Morris-Cohen, A. J.; Knowles, K. E.; Weiss, E. A. *J. Phys. Chem. B* **2010**, *114*, 14514–14520.
- (25) Krauss, T. D.; Peterson, J. J. *J. Phys. Chem. Lett.* **2010**, *1*, 1377–1382.
- (26) Manna, L.; Scher, E. C.; Li, L. S.; Alivisatos, A. P. *J. Am. Chem. Soc.* **2002**, *124*, 7136–7145.
- (27) Hess, B. C.; Okhrimenko, I. G.; Davis, R. C.; Stevens, B. C.; Schulzke, Q. A.; Wright, K. C.; Bass, C. D.; Evans, C. D.; Summers, S. L. *Phys. Rev. Lett.* **2001**, *86*, 3132–3135.
- (28) Oda, M.; Tsukamoto, J.; Hasegawa, A.; Iwami, N.; Nishiura, K.; Hagiwara, I.; Ando, N.; Horiuchi, H.; Tani, T. *J. Lumin.* **2007**, *122–123*, 762–765.
- (29) Asami, H.; Abe, Y.; Ohtsu, T.; Kamiya, I.; Hara, M. *J. Phys. Chem. B* **2003**, *107*, 12566–12568.
- (30) Myung, N.; Bae, Y.; Bard, A. J. *Nano Lett.* **2003**, *3*, 747–749.
- (31) Oda, M.; Hasegawa, A.; Iwami, N.; Nishiura, K.; Ando, N.; Nishiyama, A.; Horiuchi, H.; Tani, T. *Coll. Surf. B* **2007**, *56*, 241–245.
- (32) Oda, M.; Hasegawa, A.; Iwami, N.; Nishiura, K.; Ando, N.; Nishiyama, A.; Horiuchi, H.; Tani, T. *J. Lumin.* **2007**, *127*, 198–203.
- (33) Simurda, M.; Nemeč, P.; Trojaneč, F.; Maly, P. *Thin Sol. Films* **2004**, *453–454*, 300–303.
- (34) Lee, S. F.; Osborne, M. A. *ChemPhysChem* **2009**, *10*, 2174–2191.
- (35) Krauss, T. D.; Brus, L. E. *Phys. Rev. Lett.* **1999**, *83*, 4840–4843.

- (36) Zhelev, Z.; Jose, R.; Nagase, T.; Ohba, H.; Bakalova, R.; Ishikawa, M.; Baba, Y. *J. Photochem. Photobiol. B* **2004**, *75*, 99–105.
- (37) Empedocles, S. A.; Norris, D. J.; Bawendi, M. G. *Phys. Rev. Lett.* **1996**, *77*, 3873–3876.
- (38) Shen, M. Y.; Oda, M.; Goto, T.; Yao, T. *Int. J. Mod. Phys. B* **2001**, *15*, 3574–3578.
- (39) Qu, L.; Peng, X. *J. Am. Chem. Soc.* **2002**, *124*, 2049–2055.
- (40) Leatherdale, C. A.; Kagan, C. R.; Morgan, N. Y.; Empedocles, S. A.; Kastner, M. A.; Bawendi, M. G. *Phys. Rev. B* **2000**, *62*, 2669–2680.
- (41) Ginger, D. S.; Greenham, N. C. *J. Appl. Phys.* **2000**, *87*, 1361–1368.
- (42) Fernee, M. J.; Littleton, B. N.; Rubinsztein-Dunlop, H. *ACS Nano* **2009**, *3*, 3762–3768.
- (43) Oron, D.; Kazes, M.; Shweky, I.; Banin, U. *Phys. Rev. B* **2006**, *74*, 115333/1–115333/6.
- (44) Steinfeld, J. I.; Francisco, J. S.; Hase, W. I. *Chemical Kinetics and Dynamics*; 2nd ed.; Prentice Hall: Upper Saddle River, NJ, 1998.